Imaging and Phase I Study of ^{111}In- and ^{90}Y-labeled Anti-Lewis^{Y} Monoclonal Antibody B3

Lee H. Pai-Scherf, Jorge A. Carrasquillo, Chang Paik, Otto Gansow, Millie Whatley, Deb Pearson, Keith Webber, Michael Hamilton, Carmen Allegra, Martin Brechbiel, Mark C. Willingham, and Ira Pastan[1]

Laboratory of Molecular Biology [L. H. P-S., I. P.], Department of Nuclear Medicine, Warren G. Magnuson Clinical Cancer Center [J. A. C., C. P., M. W.], Medicine Branch [D. P., M. H., C. A.], Chemistry Section, ROB [O. G., M. B.], National Cancer Institute, NIH, Bethesda, Maryland 20892; Food and Drug Administration, Bethesda, Maryland 20892 [K. W.]; and Department of Pathology, Wake Forest University, Winston-Salem, North Carolina 27157 [M. C. W.]

ABSTRACT

B3 is a murine monoclonal antibody (mAb) that recognizes a Lewis^{Y} carbohydrate antigen present on the surface of many carcinomas. An imaging and Phase I trial was performed to study the ability of ^{111}In-mAb B3 to image known metastasis and determine the maximum tolerated dose (MTD), dose-limiting toxicity (DLT), kinetics, and biodistribution of ^{90}Y-mAb B3. Patients ($n = 26$) with advanced epithelial tumors that express the Lewis^{Y} antigen were entered. All patients received 5 mCi of ^{111}In-mAb B3 for imaging. ^{90}Y-mAb B3 doses were escalated from 5 to 25 mCi in 5-mCi increments. ^{111}In-mAb B3 and ^{90}Y-mAb B3 were coadministered over a 1-h infusion. Definite tumor imaging was observed in 20 of 26 patients. Sites imaged included lung, liver, bone, and soft tissues. The MTD of ^{90}Y-mAb B3 was determined to be 20 mCi. The DLTs were neutropenia and thrombocytopenia. Tumor doses ranged from 7.7 to 65.1 rad/mCi. ^{111}In- and ^{90}Y-mAb B3 serum pharmacokinetics ($n = 23$) were found to be similar. The amount of B3 administered (5, 10, and 50 mg) did not alter the pharmacokinetics. Bone marrow biopsies ($n = 23$) showed 0.0038 ± 0.0016% of injected dose/gram for ^{111}In-mAb B3 compared to 0.0046 ± 0.0017% of injected dose/gram for ^{90}Y-mAb B3 ($P = 0.009$). When given to patients with carcinomas that express the Lewis^{Y} antigen, ^{111}In-mAb B3 demonstrated good tumor localization. The MTD of ^{90}Y-mAb B3 is 20 mCi, with myelosuppression as the DLT. Higher doses of radioactivity need to be delivered to achieve an antitumor effect. Humanized mAb B3 is being developed for evaluation in radioimmunotherapy. A clinical trial to explore the use of higher doses of ^{90}Y-mAb B3 with autologous stem cell support is planned.

INTRODUCTION

The use of radiolabeled mAbs[2] for radioimmunotherapy has been evaluated extensively in hematological malignancies and in some epithelial cancers (1, 2). Whereas therapeutic responses have been observed in patients with lymphoma and leukemia (3–6), results in patients with epithelial tumors have been disappointing (7–9). These poor responses are generally attributed to limitations in antibody delivery and unfavorable tumor dosimetry. Tumor dose is affected by the delivery of radiolabeled antibody, which is in turn dependent on physical barriers to antibody delivery (10, 11), antigen density, and physical characteristics of the radionuclide (12).

In this study, we determined whether mAb B3, a murine IgG1κ that reacts with the Lewis^{Y} carbohydrate epitope (B3 antigen; Ref. 13), would serve as a target for radioimmunotherapy. This epitope is present on a large number of glycoproteins and is abundantly and uniformly expressed by most carcinomas, including >95% of colorectal cancer, 80% of breast cancer, and 60% of non-small cell lung cancer as well as esophageal, gastric, pancreatic, ovarian, and bladder carcinomas. In contrast, mAb B3 has limited reactivity with normal tissues. mAb B3 has been chemically linked to a truncated form of *Pseudomonas* exotoxin to form immunotoxin B3-LysPE38 (LMB-1). In a Phase I clinical trial, LMB-1 was given to 38 cancer patients with tumors that react with mAb B3. In that study, five objective responses (1 complete remission, 1 partial remission, and 3 minor responses) were observed (14), indicating that the B3 antigen can be used as target for cancer therapy.

To explore the usefulness of B3 antigen as a target for radioimmunotherapy, preclinical experiments were conducted. When injected into immunodeficient mice bearing a human epidermoid carcinoma that expresses the B3 antigen, ^{111}In-B3 showed selective and progressive accumulation at the tumor site (15). These results and preclinical biodistribution studies using ^{88}Y-mAb B3 (16, 17) indicated that radiolabeled B3 warrants further clinical evaluation.

Whereas the largest number of radioimmunotherapy studies have focused on using ^{131}I-labeled antibodies, several limitations have been identified, including rapid dehalogenation

Received 6/8/99; revised 2/7/00; accepted 2/16/00.
The costs of publication of this article were defrayed in part by the payment of page charges. This article must therefore be hereby marked *advertisement* in accordance with 18 U.S.C. Section 1734 solely to indicate this fact.

[1] To whom requests for reprints should be addressed, at Laboratory of Molecular Biology, National Cancer Institute, Building 37, Room 4E16, 37 Convent Drive MSC 4255, Bethesda, MD 20892-4255. Phone: (301) 496-4797; Fax: (301) 402-1344.

[2] The abbreviations used are: mAb, monoclonal antibody; HSA, human serum albumin; % ID, percentage of injected dose; HAMA, human antimouse antibody; AUC, area under the curve; MTD, maximum tolerated dose; SPECT, single-photon emission computed tomography; ANC, absolute neutrophil count; CT, computed tomography; DLT, dose-limiting toxicity.

(18, 19) and emission of high-energy γ-rays, which imposes certain radiation safety constraints. ^{90}Y has been evaluated as an alternative to ^{131}I for radioimmunotherapy because of its ready availability from a ^{90}Sr/^{90}Y generator (20) and its physical and biological characteristics (21–24). Whereas ^{90}Y has favorable characteristics for therapy [$t_{1/2}$ = 64 h; pure β-emission (E_{max} = 2.28 MeV)], the lack of γ-ray emission makes it suboptimal for imaging and assessing biodistribution (12). To trace the biodistribution of ^{90}Y, ^{111}In has been used as a surrogate marker because it has similar coordination chemistry (25, 26) and metabolic handling (19, 22). In this study, we carefully compared the differences in biodistribution between ^{111}In- and ^{90}Y-labeled B3. Prior studies using weaker chelates have shown significant differences between ^{111}In and ^{90}Y (23, 24). Newer chelates have greater *in vitro* and *in vivo* stability (16, 27, 28). Nevertheless, even with improved chelates, some differences between ^{111}In and ^{90}Y have been observed (17, 24). Using a different antibody labeled with ^{111}In and ^{90}Y via the 1B4M chelate (also known as Mx-diethylenetriamine pentaacetic acid; Ref. 27) in patients with adult T-cell leukemia (3), we have previously shown that there are differences in biodistribution between these two radiolabels, although these differences were small (29). Other investigators have also used the same chelate conjugate to label other antibodies (30–32); nevertheless, this is the first detailed pharmacokinetic comparison of these two isotopes using this chelate in epithelial tumors.

This study presents the results of a clinical trial in patients with advanced carcinomas that express the B3 antigen. We studied the ability of ^{111}In-1B4M-mAb B3 to image known metastasis and performed a Phase I trial to determine the toxicities, pharmacokinetics, and the MTD of ^{90}Y-1B4M-mAb B3.

MATERIALS AND METHODS

B3 mAb. mAb B3 is a murine IgG1 developed as described previously (13). The mAb B3 used for this clinical trial was purified by Verax Co. (Lebanon, NH) from low serum culture medium using ion-exchange chromatography. It was over 95% pure as established by SDS-PAGE.

Conjugation and Labeling. The B3 mAb was conjugated to 2-(4-isothiocyantobenzyl)-6-methyl-diethylenetriamine pentaacetic acid (1B4M-diethylenetriamine pentaacetic acid; Ref. 27). Radiolabeling was performed with pharmaceutical grade ^{111}In (DuPont New England Nuclear, Wilmington, DE) for imaging and/or pharmaceutical grade ^{90}Y for therapy (DuPont New England Nuclear). In brief, 1.0–1.2 mg of conjugated mAb B3 was put into a polypropylene vial that served as the reaction vessel. For ^{111}In, 10.2–23.2 mCi were added to the reaction vessel and allowed to react for 1 h. For ^{90}Y labeling, the starting amount of radioactivity and antibody dose depended on the dose level to be used. Typically, 8.9–53.3 mCi of ^{90}Y were incubated with 1.08–4.31 mg of the conjugate for 15 min. After the initial eight patients' ^{90}Y labeling, the method was modified to add ascorbate (11 mg/0.05 ml) as a radioprotectant during the incubation with ^{90}Y. Excess DTPA (10^{-4} M) was then added to the incubation mixtures to form complexes with unreacted ionic isotope. The mAb B3-bound fraction was separated by preparative size-exclusion high-performance liquid chromatography (3). Purification resulted in a final product with >99% antibody-bound ^{111}In or ^{90}Y. The ^{90}Y fraction was mixed with 25% HSA to yield a 2.5% HSA solution. Purity was determined by instant thin-layer chromatography using silica gel-impregnated glass fiber sheets (2:2:1, 10% ammonium formate in water/methanol/0.2 M citric acid) and paper chromatography using saline solvent and Whatmann #1 paper pretreated with 5% HSA. The final product was filtered using a sterile 0.22-μm low-protein-binding filter (Millex-GV; Millipore, Inc., Bedford, MA). The specific activities of the ^{111}In-mAb B3 doses (n = 26) ranged from 4.3–13.0 mCi/mg (7.3 ± 1.8 mCi/mg). The total ^{111}In activity injected ranged from 3.5–5 mCi. The specific activities of the ^{90}Y-mAb B3 doses (n = 23) ranged from 5.3–12.9 mCi/mg (8.4 ± 1.7 mCi/mg), with individual doses of 5–25 mCi of ^{90}Y-mAb B3. All products passed sterility and pyrogen testing. The ^{111}In-labeled products were injected within 72 h of preparation. Twenty-two of 23 ^{90}Y-mAb B3 doses were injected the day of labeling, whereas one product was injected the next day (24 h). The dose injected the day after labeling was retested before injection and showed similar protein-bound radioactivity.

The immunoreactivity of the radiolabeled products was tested using a modification of the cell-binding assay described by Lindmo *et al.* (33). In brief, an increasing number of A431 cells were incubated in 6-well plates in cell numbers ranging from 4×10^5 to 1×10^6. A small fixed amount of the radiolabeled B3 was added to the wells and incubated for 2 h. After incubation, the wells were washed, and the percentage of activity bound to cells was determined. Overall, the cell binding assay for the ^{111}In and ^{90}Y preparations was not significantly different, with a mean ± SD of 69 ± 10% and 69 ± 17% for ^{111}In- and ^{90}Y-mAb B3, respectively. When the immunoreactivity from ^{90}Y preparations labeled in the absence of ascorbic acid were compared with those labeled in the presence of ascorbic acid, a significant difference was observed (58 ± 10% and 74 ± 18%, respectively).

Patient Selection. Adult patients with metastatic gastrointestinal tract, breast, non-small cell lung, bladder, and ovarian carcinoma who had failed standard therapy were eligible for this study. Tumors expressed B3 antigen on ≥30% of the tumor cells as determined by immunohistochemistry. Tumor histology was confirmed by a NIH pathologist. Other eligibility criteria included: (*a*) advanced unresectable disease; (*b*) failed conventional chemotherapy; (*c*) Eastern Cooperative Oncology Group performance status of ≤2; (*d*) a minimum life expectancy of 3 months; (*e*) serum creatinine < 1.6 mg/dl; (*f*) serum bilirubin < 1.5 mg/dl; (*g*) absolute neutrophil count (ANC) > 2,000/mm^3; and (*h*) platelets > 100,000/mm^3. Patients with clinically significant cardiac disease (New York Heart Association grade 3 or 4) were excluded, as were those with infectious disease that required antibiotic therapy, brain metastasis, prior exposure to murine antibodies, pregnancy, or lactation. Patients who had received bone marrow transplant therapy, more than 3 chemotherapy regimens, pelvic radiation, or local radiation to more than one site were excluded. The clinical protocol and the consent form were approved by the Institutional Review Board of the National Cancer Institute. Informed consent was obtained from all patients before participation in this study.

Study Design. An outline of the protocol design and the number of patients entered in each group are shown in Table 1. In the initial portion of this study, three patients received 5 mCi

Table 1 Protocol outline

Imaging (^{111}In-B3) (mCi)	Therapy (^{90}Y-B3) (mCi)	Total B3 (mg)	*n*
5	5 (optional)	5	3
5	5	5	3
5	5	10	3
5	5	50	3
5	10	10	3
5	15	10	3
5	20	10	6
5	25	10	2

of ^{111}In-mAb B3. The objective was to determine whether there would be any gross unexpected sites of localization of the antibody or acute toxicities that would prompt us not to proceed with the therapy portion of the study. To provide potential therapeutic benefit, these initial patients were offered therapy with 5 mCi of ^{90}Y-mAb B3, if they had tumor imaging, no HAMAs, and no toxic side effects or unexpected, undesirable tissue accumulation as compared with other ^{111}In-labeled antibodies. In the second portion of the study, we evaluated whether the amount of antibody resulted in dose-dependent changes in biodistribution. Three groups of three patients each received ^{111}In (5 mCi)- and ^{90}Y-mAb B3 (5 mCi) mixed together with 5, 10, or 50 mg of unlabeled mAb B3. In the third and main part of the protocol, the MTD of ^{90}Y was determined. Groups containing three patients each received escalating doses of ^{90}Y-mAb B3 for therapy coinfused with 5 mCi of ^{111}In and a total of 10 mg (based on a lack of dose-dependent changes at the higher amounts of mAb B3). The ^{90}Y doses were escalated in 5-mCi intervals. Patients with hematological toxicity $<$ grade 3 were eligible for retreatment with the same dose of ^{90}Y if they had no evidence of disease progression and remained HAMA negative.

^{111}In-mAb B3 and ^{90}Y-mAb B3 were coadministered i.v. over a 1-h infusion in an outpatient setting.

Pharmacokinetics. Intravascular kinetics were determined by counting ^{111}In or ^{90}Y radioactivity in blood and plasma aliquots obtained at the following times after the end of infusion: 5 min, 30 min, 1 h, 2 h, 6 h, 1 day, and daily for up to 7 days after the end of the infusion. The % ID/ml was obtained by comparing the counts to a standard of the injected dose. The plasma and blood volumes were estimated at each time of treatment using a nomogram based on body surface area (34). Using the latter estimated volumes and the % ID/ml, the total % ID in the blood and plasma volume was calculated. Because the infusion time was short compared with the disposition half-life ($t_{1/2}$), the intravascular data were treated similar to an i.v. bolus. The % ID/ml of blood or plasma was fitted to a biexponential curve to obtain both the α and β phase $t_{1/2}$ using a least-squares fit algorithm. Conventional pharmacokinetic parameters were then derived (35). The AUCs for the blood or plasma curves were calculated in two steps. First, the AUC from the end of antibody infusion (*To*) to 168 h was obtained by trapezoidal integration of the decay-corrected blood and plasma data, and then the terminal AUC was estimated using the terminal clearance rate to extrapolate from the activity retained at the last measured time point. Using this data, we then estimated additional pharmacokinetic parameters, including volume of distribution, clearance, and half-life (35). Serial 24-h urine collections were obtained for up to 96 h so that we could compare the urinary excretion of the two tracers. Whole body clearance of ^{111}In was determined from the imaging data (see below).

Imaging. Scintillation camera images were first recorded up to six times with a large field of view dual-headed gamma camera starting within ~2 h of the end of the infusion and daily for up to 6 or 7 days. Analogue and digital images of anterior and posterior whole body as well as spot views (5–10 min/image) were obtained. For quantitative imaging, a 20% window centered over the 247 keV photopeak of ^{111}In was obtained. A scatter correction method was utilized. The images were corrected for attenuation using a ^{99m}Tc flood source and allowing for the energy differences and the sensitivity of the gamma camera. A geometric mean image was then generated (in units of μCi/pixel). For visual interpretation, individual anterior and posterior images were reviewed. SPECT of the chest, abdomen, and pelvis was recorded using a medium energy collimator; SPECT was typically performed 4 to 5 days after injection. The ^{111}In SPECT images were obtained for visual assessment utilizing a 20% window centered over the 174 and 247 keV photopeak of ^{111}In; the images were reconstructed using a Hamming filter with a high cutoff frequency of 0.75 cycle/cm. All images were interpreted by one experienced nuclear medicine physician.

Two quantitative image regions of interest were drawn over the liver, spleen, and L4 vertebral body on the geometric mean images. The integrated radioactivity in the organs (AUC) was then determined by trapezoidal integration up to the last time point imaged (typically 7 days), and the remaining AUC was determined by extrapolation using the terminal $t_{1/2}$ of clearance. The whole body $t_{1/2}$ was obtained by fitting the geometric mean concentration of ^{111}In activity of the anterior and posterior whole body scans. Using the residence times obtained from the data above and the individual organ size, as determined from CT, the medical internal radiation dose method was used to calculate organ dosimetry (36). In brief, the integral of radioactivity in a given organ, blood, or tissue was divided by its weight (μCi·h/g) and multiplied by the mean energy emitted per nuclear transition of the β particle from ^{90}Y (1.99 g·Rad/μCi/h), assuming an absorbed dose fraction of 1. The activity in L4 was determined from the region of interest analysis and integrated over time. This activity was normalized by the grams of bone marrow in L4 as estimated in standard man (37). The dose to the bone marrow was then estimated as described above.

Counting Methods. Dual isotope counting of ^{111}In and ^{90}Y was performed on the patient samples. The ^{111}In γ-ray peaks were counted in a gamma counter using a 100–500 keV energy setting. Because ^{90}Y is counted with $<$4% efficiency in a gamma counter, Cerenkov counting in a beta counter was also utilized. Cerenkov counting was performed using an energy range of 0–200 keV (A4530D Packard, Downes Grove, IL) in a beta counter. Because Cerenkov counting is sensitive to quench and geometry, all samples were processed in a similar and reproducible manner as described previously (29), which included solubilizing the samples with SDS and bleaching them with 30% hydrogen peroxide to minimize quench. The counts in

the samples were referred back to a standard of the injected dose that had been prepared in a similar fashion using the patients' plasma or blood to mimic the quench. The counts obtained in the gamma and beta counters were corrected for cross-talk and decay.

Bone Marrow Biopsies. Twenty-five patients underwent bone marrow biopsy of the posterior iliac spine within 5–7 days after mAb injection. Thirteen biopsies were performed 6 days after therapy, eight were performed at 5 days after therapy, and four were performed at 7 days after initial therapy. The biopsy cores were weighed on an analytical balance and put in a conical tube with 10 ml of PBS for 1 h and analyzed as described previously (29). The core was broken with a jagged-edged glass rod. This was centrifuged for 10 min at 640 × *g*, and the supernatant was removed and counted (saline fraction). The pelleted core was broken with a jagged-edged glass rod and mixed with 0.5 ml of 10% SDS. The core was heated to 56°C for 30 min in an attempt to remove any cell-bound activity. After the sample cooled, 0.4 ml of 30% hydrogen peroxide was added as bleach, and the mixture was incubated at 56°C for 1 h to bleach the sample. Ten ml of distilled water were added, and the sample was again centrifuged for 10 min. The supernatant was separated for counting (SDS fraction). Perchloric acid (0.2 ml) was then added to the remaining bone chips, and the mixture was incubated at 56°C until the bone was dissolved (bone fraction). This sample was again treated with hydrogen peroxide as described above. After cooling, the sample was transferred to a counting vial with 10 ml of distilled water. All samples were then counted in the gamma and beta counters with the appropriate decay and cross-talk corrections.

To attempt to find parameters that predict bone marrow toxicity, we correlated the dose to bone marrow based on imaging, bone marrow biopsy, and blood retention of ^{90}Y. The dose to the blood was calculated as described above, and the dose to the marrow was then determined by multiplying times the red marrow:blood ratio as described by Sgouros *et al.* (38). The dose from marrow biopsies was determined by calculating the activity concentrated in the marrow by gamma counting of a precisely weighted specimen. We assumed that there was no biological clearance from the marrow, based on gamma camera imaging. The dose was then calculated as described above, with no corrections for cortical bone. In addition, we correlated toxicity to the bone marrow with administered activity or administered activity corrected for body weight.

HAMA Assays. HAMA assay was performed as described previously using a high-performance liquid chromatography method (39). More than 10% complex formation using a ^{125}I isotype matched nonspecific mAb (BL-3) and ^{125}I-labeled B3 was considered positive.

Statistics. To compare independent data, ^{111}In and ^{90}Y patient data obtained from the initial dual-injection study were used. Paired *t* test or Wilcoxon rank signed test (when data were not normally distributed) was performed to assess the differences in biodistribution between the two radiolabels. Pearson's correlation coefficient was used to evaluate the relationship between nominal data, and Spearman correlation coefficient was used with ordinal data.

Table 2 Patient characteristics

n = 26	
Sex: 12 male, 14 female	
Age: 39–73 yrs (mean = 58)	
Tumor histology	
20 colon carcinomas	
2 esophageal cancers	
1 gastric cancer	
1 breast cancer	
1 bronchoalveolar cancer	
1 cancer of the ampulla of Vater	
Prior therapy	
Chemotherapy	
1 regimen	11 (42%)
2 regimens	10 (38%)
3 regimens	4 (15%)
Hormonal	1 (3%)
Biological (INF)[a]	6 (26%)
Radiation (1 site)	3 (11%)
No. of metastatic sites	
1 site	10 (38%)
2–3 sites	14 (54%)
≥4 sites	2 (7%)
Sites of metastasis, number of patients	
Liver, 17	
Lung, 13	
Soft tissue, 8 (perit, 4; pleura, 1; abdominal wall, 3)	
Lymph nodes, 8 (chest 2, abdomen 6)	
Bone, 3	
Stomach, 2	
Effusion, 6 (pleura, 2; ascites, 4)	

[a] INF, interferon.

RESULTS

Patient Characteristics and Clinical Observation. Twenty-six patients were entered into this study. Their clinical characteristics are shown in Table 2. There were 12 men and 14 women (age range, 39–73 years; mean age, 58 years). Twenty patients had colorectal cancer, 2 patients had esophageal cancer, 1 patient had gastric carcinoma, 1 patient had carcinoma of the ampulla of Vater, 1 patient had breast cancer, and 1 patient had bronchioalveolar cancer. Prior therapy and sites of metastasis are shown in Table 2. Immunohistochemical staining of B3 was performed on paraffin-embedded tumor blocks from the primary surgery in all cases. Homogeneous B3 expression was found in 23 of 26 patients. In 3 of 26 cases, specimens were poorly preserved (tightly fixed). However in all three cases, sections indicated that in the better preserved areas, more than 30% of the tumor cells were clearly positive for B3 antigen.

Infusion of unlabeled and radiolabeled antibody was well tolerated, accompanied by minimal or no side effects. Nonhematological toxicities were mild and transient (grade 1 and 2), with low-grade fever observed in four patients within 24 h after dosing. Rigor and chills were reported in one patient. Grade 1 arthralgia (one patient), myalgia (two patients), and fatigue (one patient) were observed at 2–4 weeks after dosing. Patients were treated with acetaminophen or ibuprofen as needed. It is unlikely that these symptoms were related to the therapy. As expected, the DLT was myelosuppression (see below). There were no significant changes in the chemistry profiles related to

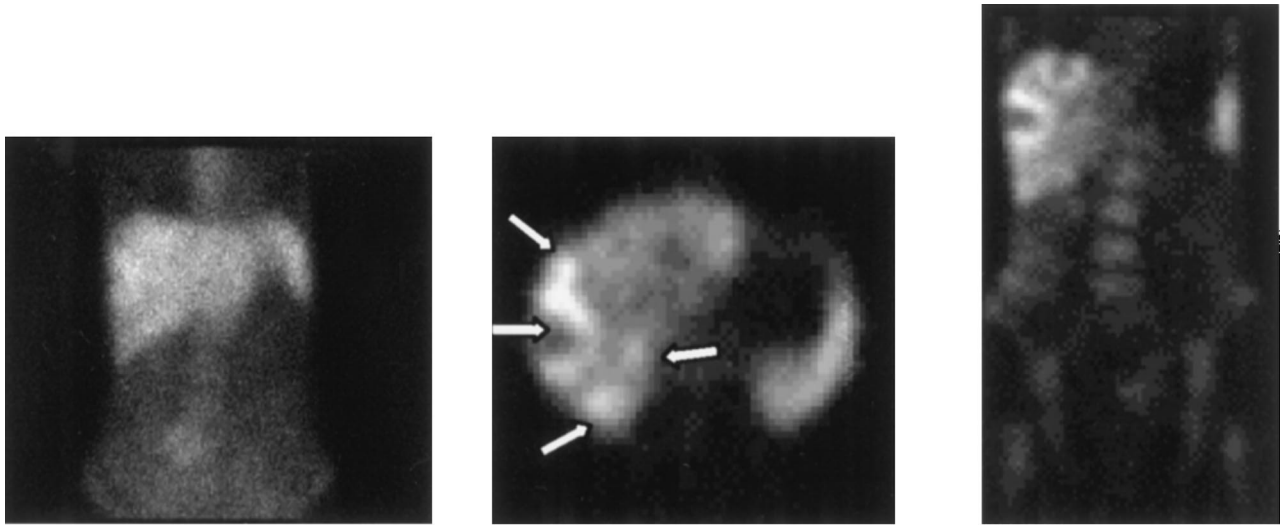

Fig. 1 ^{111}In images of a 57-year-old female with metastatic colon cancer to the liver. Images were obtained at 96 h after administration of 5 mCi of ^{111}In and 25 mCi of ^{90}Y. The *left panel* shows an anterior planar view of the abdomen, where tumor uptake is faintly visualized. The *middle* and *right panels* are a transverse and a coronal section, respectively, from a SPECT scan through the liver. The SPECT study clearly shows several focal areas of tumor uptake (*arrows*).

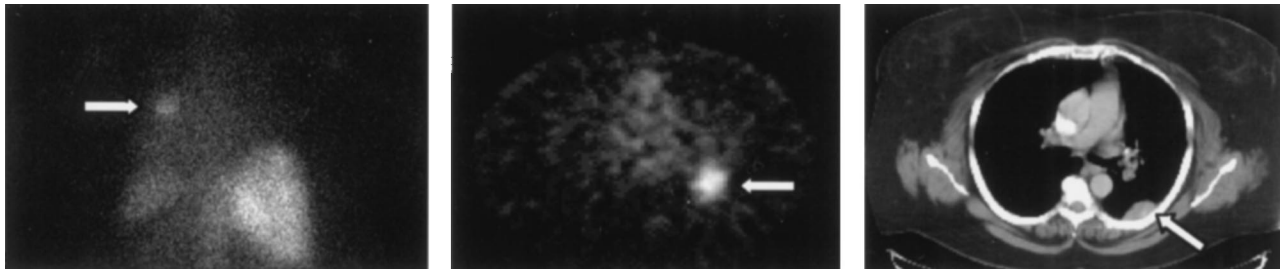

Fig. 2 Images from a 52-year-old female with metastatic colorectal cancer to the left lung. Antibody imaging was performed 120 h after i.v. administration of 5 mCi of ^{111}In and 20 mg of mAb B3 (the patient was coinjected with 20 mCi of ^{90}Y-mAb B3). The *left panel* shows a posterior planar view of the chest, showing a focal area of increased uptake in the left lung (*arrow*). The *middle panel* is a transverse SPECT through the lung lesion, and the *right panel* is the corresponding CT.

the mAb treatment. The disease status remained stable for 6 weeks in four patients. There were no clinical responses to the infusion of ^{90}Y-mAb B3.

Imaging Results. Twenty-one of 26 patients (85%) had localization in known sites of disease. Sites of disease imaged included liver (Fig. 1), lung (Fig. 2), bone, soft tissue mass, and lymph nodes. Table 3 shows the radiographic results and ^{111}In-mAb B3 imaging results of individual patients.

Seventeen patients had known liver metastasis as shown by CT scan. Several imaging patterns were noted in the liver. A total of nine patients had positive uptake in the liver: six had lesions with hot rims and cold centers (Fig. 2); whereas three patients had hot lesions. Eight patients were considered negative and had either no localization or lesions that appeared cold and had some filling in on delayed imaging but were never hotter than the normal liver.

Normal sites of ^{111}In accumulation included the liver, spleen, and bone marrow (Fig. 1). Excretion into the urinary bladder and occasional mild bowel uptake were seen. Bowel activity moved over time, indicating that it represented intraluminal activity. No gall bladder uptake was visualized. Delayed images showed progressive clearance of the blood pool and persistent accumulation in the liver and bone marrow. Lesions were better visualized on SPECT scans than on planar images (Figs. 1 and 2). No gross differences in imaging were observed at the various dose levels to suggest dose-dependent changes in biodistribution.

Pharmacokinetics. The administered mass of mAb B3 did not have a significant effect on pharmacokinetic parameters for ^{111}In (Table 4). No significant differences in plasma pharmacokinetics were observed between ^{111}In- and ^{90}Y-mAb B3 (Table 5). The blood and plasma clearance was very similar for both ^{111}In- and ^{90}Y-mAb B3 (Fig. 3). The amount of antibody remaining in the plasma volume at the end of infusion was 80.7 $\pm$ 6.1, 86.7 $\pm$ 10.6, and 90 $\pm$ 7.6% ID for the 5, 10, and 50 mg dose of ^{111}In-mAb B3, respectively (ANOVA, P = 0.43). At 168 h after infusion, the amount of ^{111}In-mAb B3 remaining in the plasma volume was 12.3 $\pm$ 2.0, 11.8 $\pm$ 3.0,

Table 3 Radiographic and ^{111}In-mAb B3 imaging results

Patient	Radiographic results	^{111}In imaging results
1	Lung	Lung +
	Liver	Liver − (fill in only)
		Abdomen false + (bowel)
2	Lung	Lung +
	Liver	Liver − (cold center)
3	Lung	Lung +
	Bone	Bone +
	Mediastinum/hilar LN[a]	Mediastinum +/ hilar +
4	Liver	Liver − (cold center)
	Periaortic LN	Periaortic +
5	Pancreatic mass	Pancreatic mass −
6	Liver	Liver + (hot rim)
7	Bone (rib)	Bone +
	Lung (0.5 cm)	Lung nodule −
		Presaccral area false +
8	Pleura (RLL)	Pleura +
	Liver	Liver −
	Retroperitoneal LN	Retroperitoneal LN −
	EG junction mass	EG junction mass −
9	Liver	Liver − (fill in)
10	Liver	Liver + (hot rim)
	Periportal LN	Periportal LN −
	Presaccral mass	Presaccral mass +
11	Abdominal wall	Abdominal wall +
12	Liver	Liver − (fill in)
13	Lung	Lung +
	Hilar LN	Hilar LN −
14	Liver	Liver − (fill in)
15	Lung	Lung +
	Liver	
16	Lung	Lung +
17	Liver	Liver + (hot rim)
	Lung	Lung +
	Retroperitoneal LN	Retroperitoneal LN −
	Ascites	Ascites +
18	Liver	Liver + (hot rim)
	Pelvic mass	Pelvic mass +
	Perihepatic mass	Perihepatic mass +
	Ascites	Ascites +
19	Abdominal wall mass	Abdominal wall mass +
	Liver	Liver − (cold lesions)
	Lung	Lung −
	Retroperitoneal LN	Retroperitoneal LN −
	Ascites	Ascites +
20	Stomach (linitis plastica)	Stomach −
	Ascites	Ascites +
21	Liver	Liver + (hot rim, some cold)
	Peritoneal mass	Peritoneal mass +
22	Liver	Liver + (hot rim)
	Retroperitoneal LN	Retroperitoneal LN −
23	Liver	Liver + (hot lesions)
	Lung	Lung +
	Pleura	Pleura +
24	Liver	Liver + (hot lesions)
	Bone	Bone +
	Pleural effusion	Pleural effusion −
25	Liver	Liver + (hot rim)
	Mesentery mass	Mesenteric mass +
26	Lung	Lung +

[a] LN, lymph node; RLL, right lower lobe; EG, esophageal-gastric.

and 12 ± 1.6% ID, for the 5, 10, and 50 mg dose, respectively (ANOVA, $P = 0.96$).

Antibody dose did not result in significant differences in the 0–96-h urinary excretion of ^{111}In or ^{90}Y. Patients receiving 5 ($n = 3$), 10 ($n = 17$), or 50 mg ($n = 3$) of mAb B3 showed a median urinary excretion (0–96 h) of 11.9%, 15.1%, and 12.2%, respectively (Kruskal-Wallis one-way ANOVA, $P = 0.26$). Similarly, the median urinary excretion of ^{90}Y at the corresponding time and doses was 9.7%, 11.1%, and 8.3%, respectively ($P = 0.06$).

The amount of ^{90}Y injected did not affect the urinary excretion (0–96 h) of ^{90}Y. Patients receiving ~5 ($n = 3$), 10 ($n = 3$), 15 ($n = 3$), or 20 mCi ($n = 6$) showed no significant differences in urinary excretion of ^{90}Y with 8.5 ± 2.2, 11.1 ± 1.0, 18.9 ± 15.1, and 13.3 ± 3.7% ID excreted in 96 h, respectively (ANOVA, $P = 0.35$).

The urinary excretion of ^{111}In and ^{90}Y in the interval collected is shown in Table 6. The urinary excretion of ^{90}Y in the first 24 h was greater than that of ^{111}In [3.9 ± 1.6% compared with 3.4 ± 1.3% ID, respectively ($P = 0.016$)]. However, at 48–96 h, the urine excretion of ^{90}Y was less than that of ^{111}In [8.0 ± 4.8% ID excreted compared with 12.3 ± 6.3% ID, respectively ($P = 0.016$)].

Hematological Toxicity. The dose and the hematological toxicity in individual patients are shown in Table 7. Hematologic DLT for this study was defined as an ANC < 500/μl for >5 days or platelets < 25,000/μl for >5 days. At doses of 5 and 10 mCi of ^{90}Y-mAb B3, minimal to no hematological toxicity was observed. Grade 2 and grade 3 thrombocytopenia were observed at 15 and 20 mCi of ^{90}Y-mAb B3. One instance of DLT occurred in one patient at 20 mCi of ^{90}Y (patient 21); as a result, a total of six patients was treated at this dose level. Dose-limiting neutropenia and thrombocytopenia occurred in two patients who received 25 mCi of ^{90}Y (patients 25 and 26). Grade 4 neutropenia (absolute granulocyte count < 500) was observed at day 28 after dosing and lasted 5 and 18 days. One patient required hospital admission and i.v. antibiotics for fever. Both patients received granulocyte colony-stimulating factor. Grade 4 thrombocytopenia (platelets = 25,000/μl) requiring platelet transfusion was observed at 18 and 25 days after dosing, lasting 42 days in one patient and 11 days in another patient.

In an attempt to obtain parameters that would predict toxicity, correlation of various indices of administered activity or bone marrow dose was correlated to either a percentage drop in WBC, ANC, or platelets or to toxicity grade in these parameters (Table 8). With the exception of estimates of bone marrow dose from imaging, the majority of the parameters showed a good correlation with changes in peripheral blood counts. The correlation of drop in blood counts or bone marrow toxicity based on the dose (mCi) administered correlated in the same range as the other parameters that corrected the dose (mCi) based on weight. The estimates of bone marrow dose based on the blood radioactivity or the ^{90}Y accumulation in the bone marrow biopsy were in the same range and were not better predictors of toxicity than the administered activity.

Bone Marrow. The dose of antibody (mg) did not alter the localization of radioactivity in the bone marrow. The mean concentration of ^{111}In in the bone marrow was not significantly different for the 5, 10, or 50 mg doses and had a mean of 0.0043, 0.00391, and 0.00554% ID/g (ANOVA, $P = 0.516$). Similarly, no significant difference in the concentration of ^{90}Y was seen in the bone marrow.

The concentration of radioactivity in the bone marrow did

Table 4 Pharmacokinetic parameters for ^{111}In-mAb B3: effects of antibody mass

mAb B3 mass (mg)	5 mg	10 mg	50 mg	*P*
No. of patients	6	17	3	
AUC (% ID·h/ml	2.25 ± 0.76	2.18 ± 0.85	2.03 ± 0.31	0.93[a]
Clearance (ml/h)	49.6 ± 18.5	54.6 ± 25.3	50.1 ± 7.8	0.88[a]
$t_{1/2}$ β (h)	67.2 ± 16.5	74.4 ± 46.5	75.9 ± 3.9	0.50[b]
Vc (ml)	3259 ± 358	3164 ± 770	3695 ± 806	0.49[a]

[a] *P* determined by ANOVA.
[b] *P* determined by Kruskal-Wallis test.

Table 5 Pharmacokinetic parameters based on ^{111}In *versus* ^{90}Y

	^{111}In-mAb B3	^{90}Y-mAb B3	*P*
No. of patients	23	23	
AUC (% ID·h/ml)	2.23 ± 0.77	2.23 ± 0.81	0.21[a]
Clearance (ml/h)	51.8 ± 22.6	51.2 ± 22.9	0.15[b]
$t_{1/2}$ β (h)	74.7 ± 40	77.3 ± 43	0.06[b]
Vc (ml)	3215 ± 734	3227 ± 736	0.49[b]

[a] Wilcoxon signed rank test.
[b] *P* determined by paired *t* test.

not vary depending on the dose of ^{90}Y administered. The mean activities of ^{111}In in the bone marrow for the 5, 10, 15, 20, and 25 mCi doses were not significantly different with a mean of 0.0039, 0.0029, 0.004, 0.0027, and 0.0044% ID/g, respectively (ANOVA, $P = 0.123$). Similarly the % ID/g of ^{90}Y in the bone marrow was not affected by the administered dose (ANOVA, $P = 0.56$).

The concentration of ^{111}In in the bone marrow was lower than that for ^{90}Y in the 17 patients receiving 10 mg of antibody with escalating doses of ^{90}Y. The concentration of ^{111}In was 0.0034 ± 0.0015% ID/g, whereas that for ^{90}Y was 0.0047 ± 0.0015% ID/g. The distribution of the ^{111}In and ^{90}Y in the compartments of the bone measured (saline, SDS, and bone) were different for ^{111}In and ^{90}Y (Fig. 4).

On processing of the bone marrow, only a small proportion of the activity was lost due to processing. In the case of ^{111}In, we recovered a mean of 95 ± 15% of the nonprocessed biopsy. In contrast, because of improved efficiency of bremmstrahlung generation after processing, the ^{90}Y apparent recovery (efficiency) was 134 ± 29% of the original activity.

Dosimetry. The doses to liver, spleen, bone marrow, and tumor were estimated based on the ^{111}In biodistribution. The mean dose to the liver and spleen was 19.4 ± 4.5 and 22.2 ± 8.6 rad/mCi, respectively. The maximum total dose to the liver in this study was 576 rad, and the maximum total dose to the spleen was 716 rad. The dose to the bone marrow based on the AUC of blood was 4.8 ± 1.6 rad/mCi, and the marrow dose estimated from the biopsy was 8.3 ± 3.1 rad/mCi. Many of the tumors visualized were very extensive and overlapped with other tumor or normal structures; in some cases, their size could not be determined. The doses to tumors were variable and ranged from 7.7–65.1 rad/mCi. The mean dose to tumor was 25.1 ± 18.3 rad/mCi.

Tumor Response. No tumor responses were observed in this study. Stable disease was seen in 6 of 24 patients. No patient could be retreated because all patients developed HAMA response within 5–6 weeks after dosing.

DISCUSSION

During the past decade, several tumor-specific carbohydrate antigens have been identified (40). Because of their abundant expression on the surface of many epithelial cancers and their relative tissue specificity, surface carbohydrates such as Lewis^Y are ideal for targeted therapy. Clinical trials in cancer patients have been conducted using anti-Lewis^Y antibodies linked to toxins (14) or chemotherapy agents (41). In this study, we examined the imaging, toxicities, and pharmacokinetics of an anti-Lewis^Y antibody termed B3 labeled with radionuclides ^{111}In and ^{90}Y.

We have shown here that ^{111}In-mAb B3 has good sensitivity for imaging metastatic epithelial carcinomas that express the Lewis^Y antigen. Twenty-one of 26 patients had positive uptake of ^{111}In-mAb B3, as shown by planar and SPECT imaging. Sites imaged included lung, liver, bone, soft tissue masses, and lymph nodes. The ability of ^{111}In-mAb B3 to detect known sites of metastasis was most effective when the tumor was localized in soft tissues, in particular, the peritoneal cavity and the abdominal wall. In this location, strong, localized uptake of ^{111}In-mAb B3 was observed in eight of eight patients. This is particularly important if the agent is to be used in the setting of occult recurrences in colorectal carcinomas, ovarian carcinomas, and other gastrointestinal malignancies. Although the accumulation of ^{111}In in the normal liver tissue makes it difficult to develop tumor€background ratios high enough to detect the malignancy, clear positive uptake was observed in 9 of 17 patients with liver metastasis. Four different patterns were observed. In some cases, the liver metastasis presented as hot lesions, whereas others had lesions with a hot rim and cold centers. Some lesions that were considered negative had either no localization or had lesions that appeared cold; however, on delayed imaging, these lesions showed some filling in but were never hotter than the normal liver. It is possible that these represent areas of necrosis and/or poor vascularization (42–44). Failure of ^{111}In-mAb B3 to detect all tumors in this study could be due to nonhomogeneous expression of the B3 antigen in the metastatic sites or poor vascularization. It is also possible that a number of lesions detected by radiographic imaging represent reactive lymph nodes or fibrotic tissue.

The usefulness of mAb B3 as an imaging agent would need to be further evaluated in larger clinical studies in patients with small volume disease (*e.g.*, patients with elevated carcinoembryonic antigen or CA-125 with no radiographic evidence of disease). However, the tumor localization of B3 observed in this first trial indicates that the use of this antibody as a radiotherapeutic agent warrants further investigation.

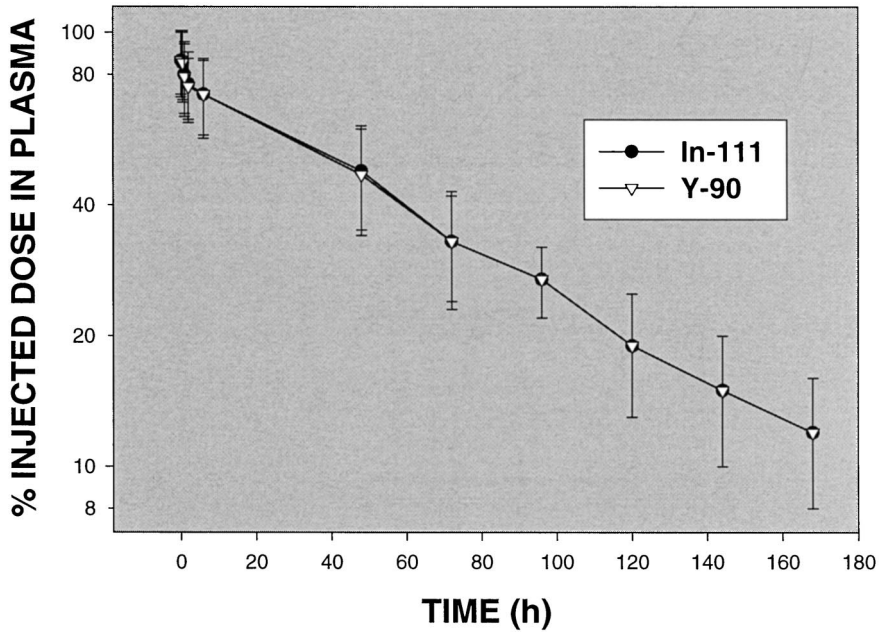

Fig. 3 The % ID of ^{111}In-mAb B3 in the plasma volume was determined (see "Materials and Methods"). ^{111}In and ^{90}Y intravascular retention is very similar, although small differences were seen. The data are plotted as the mean ± SD from all 23 patients undergoing paired studies.

Table 6 Urinary excretion of ^{111}In and ^{90}Y after coinfusion of ^{111}In and ^{90}Y-mAb B3

Time (h)	Paired studies ^{111}In % ID excreted	Paired studies ^{90}Y % ID excreted	*P*
0–2	0.9 ± 0.5	1.15 ± 0.65	<0.001[a]
2–24	2.5 ± 1.1	2.72 ± 1.25	0.137[b]
24–48	3.7 ± 2.1	2.75 ± 1.74	<0.001[b]
48–72	4.3 ± 2.9	2.76 ± 2.17	<0.001[a]
72–96	4.3 ± 2.2	2.51 ± 1.37	<0.001[a]
0–24	3.4 ± 1.3	3.87 ± 1.63	0.016[b]
24–96	12.3 ± 6.3	8.02 ± 4.82	<0.001[b]

[a] *P* determined by signed rank test for nonnormally distributed data.

[b] *P* determined by paired *t* test.

Table 7 Hematological toxicity

Patient	Dose ^{111}In-B3 (mCi)	Dose ^{90}Y-B3 (mCi)	Dose B3 (mg)	Myelosuppression grade AGC[a]	Myelosuppression grade Platelets
1	5		5		
2	5		5		
3	5	5	5		
4	5	5	5		
5	5	5	5		
6	5	5	5		1
7	5	5	10	1	
8	5	5	10		
9	5	5	10		
10	5	5	50		
11	3.7	5	50		
12	5	5	50		
13	5	10	10	3	1
14	5	10	10		
15	5	10	10		
16	5	15	10	2	2
17	5	15	10		1
18	5	15	10		1
19	5	20	10		3
20	5	20	10	3	1
21	5	20	10	3	4
22	5	20	10		1
23	5	20	10		1
24	4.2	20	10		
25	5	25	10	4	4
26	5	25	10	4	4

[a] AGC, absolute granulocyte count.

The use of ^{90}Y-labeled antibodies directed against lymphoma has resulted in significant objective tumor responses (3, 31, 32, 45). Response in epithelial tumors has been more difficult to attain. Several radioimmunotherapy trials using ^{90}Y have been reported previously, although the majority are preliminary reports or reports on a smaller number of patients than seen in our trial.

^{90}Y-mAb B3 is well tolerated at doses up to 20 mCi, with neutropenia and thrombocytopenia as the dose DLTs. The MTD is in the range observed by others (3, 46, 47). Our dose estimates based on marrow biopsy were in a range consistent with that at which bone marrow toxicity would be expected at the 25-mCi dose level. Toxicity could be correlated to various ^{90}Y parameters including administered dose, dose/kg, dose/m^2, and dosimetry based on blood or biopsy. The correlation to dose based on imaging was the poorest, perhaps due to the difficulty in assessing bone marrow concentration using imaging techniques. If the bone marrow were not dose limiting, our normal organ dosimetry in liver would suggest that significantly higher doses could be utilized, if one assumes that toxicity for external beam to the liver will be similar, because the $TD_{50}/5$ for liver is 2000 rad. The dosimetry estimates to tumor suggest that we could deliver doses of up to 80 mCi. The bone marrow concentration ob-

Table 8 Correlation of toxicity with administered ^{90}Y-mAb B3 dose and with bone marrow dose estimates

	% Drop			Toxicity grade		
	WBC	ANC	PLATELET	WBC	ANC	PLATELET
mCi	0.782[a]	0.724	0.815	0.712	0.561	0.685
mCi/kg	0.802	0.783	0.806	0.741	0.611	0.652
mCi/m^2	0.821	0.785	0.842	0.739	0.619	0.666
Rad dose blood	0.753	0.728	0.737	0.635	0.569	0.558
Rad dose bone marrow (biopsy)	0.757	0.695	0.785	0.666	0.567	0.586
AUC (humerus)	0.353	0.0474	0.399	0.18	0.343	0.226
AUC (L4)	0.218	0.195	0.193	0.44	0.353	0.425

[a] Pearson correlation coefficient was used for % drop data (nominal data); Spearman correlation coefficient was used for toxicity grade data (nominal data).

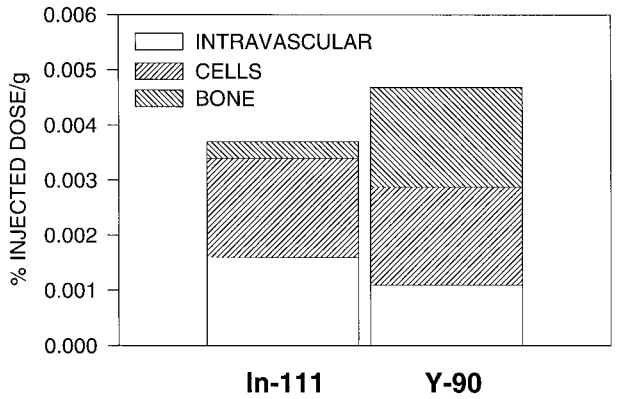

Fig. 4 Bone marrow concentrations of ^{111}In and ^{90}Y were determined. Bone marrow biopsies were processed as described in "Materials and Methods." Radioactivity in the bone marrow from ^{111}In-labeled mAb B3 is shown in the *left columns*, and radioactivity in the bone marrow from ^{90}Y is shown in the *right columns*. Radioactivity is shown in the following fractions: bone fraction (▧); SDS fraction (▨); and the intravascular fraction (□). The data are expressed as the mean concentration from patients undergoing paired ^{111}In and ^{90}Y studies.

served, based on bone marrow biopsy, is in the range of that observed with murine anti-Tac (29). The ^{111}In concentrations from mAb B3 and mAb anti-Tac in bone marrow were 0.00378 and 0.00293% ID/g, respectively ($P = 0.243$ paired t test). In addition, the concentration of ^{90}Y in the bone marrow from ^{90}Y-B3 and anti-Tac were 0.0047 and 0.00494% ID/g, respectively ($P = 0.777$, paired t test).

The blood clearance of ^{111}In- and ^{90}Y-mAb B3 is similar to that reported previously with 1B4M chelate and other second-generation chelates (29, 48); in contrast, chelates that are less stable for ^{90}Y have shown less concordance in preclinical models (16) or in clinical trials (49, 50).

The tumor doses that we delivered are in the general range of those reported by others using other ^{90}Y-labeled antibodies (49, 51). The doses to other organs are generally similar, although some antibodies may have a higher concentration in the liver and therefore result in slightly higher liver doses (51, 52). These higher liver doses may be related to the presence of circulating antigen and complex formation (51), which was not present in our system.

Halpern *et al.* (53) have previously shown that the distribution of each mAb is unique unto itself with regard to its response to the mass effect. Because this "carrier effect" can alter not just the serum half-time of an antibody but also the organ tumor distribution of the radionuclide, we administered increasing amounts of mAb B3 to patients. No dose-dependent differences in pharmacokinetics were observed at doses of 5–50 mg of mAb B3, nor were there differences in urine excretion that related to the dose administered. Pharmacokinetic analysis indicated that there were no significant differences in plasma clearance of ^{111}In- and ^{90}Y-mAb B3.

Nevertheless, significant differences in urinary excretion of ^{111}In and ^{90}Y were observed. These consisted of slightly faster excretion of ^{90}Y at the early times after injection but much higher excretion at later times. This probably reflects different handling of the radiometals, with possible excretion of some ^{111}In as catabolism occurs, which would contrast with retention of ^{90}Y, in particular, in the bone. These findings are similar to those we have reported previously with two different ^{90}Y-radiolabeled mAbs (29, 48). The preferential accumulation of ^{90}Y was evident as reflected by the bone marrow biopsy, which showed a mean of 1.4 times more ^{90}Y than ^{111}In. Using our coarse bone marrow fractionation method, it was clear that the greatest portion of ^{90}Y retained was in the bone fraction.

In summary, we have shown here that specific targeting of the Lewis^Y antigen using radionuclide linked to mAb B3 is feasible. It is clear that to achieve an objective antitumor effect, higher doses of radionuclide will need to be delivered. Strategies to improve the therapeutic index include peripheral autologous stem cell rescue to overcome the myelosuppression (54, 55) and i.v. infusion of EDTA to prevent binding of free ^{90}Y to bone (56). As in external beam radiotherapy, the use of fractionated multiple doses for delivery of ^{90}Y should also be explored. Humanized mAb B3 is presently being produced for evaluation in radioimmunotherapy. This should overcome the problem with HAMA formation. A clinical trial to explore the use of a higher dose of ^{90}Y-mAb B3 with autologous stem cell support is being planned at the National Cancer Institute.

ACKNOWLEDGMENTS

We thank Debby Drumm for expert technical assistance with binding assays and handling of patient samples. We also thank Nhat Le and Mark Rotman for expert technical assistance labeling the antibodies and Craig Barker for expert technical assistance with setting up the quantitative imaging.

REFERENCES

1. Wilder, R. B., DeNardo, G. L., and DeNardo, S. J. Radioimmunotherapy: recent results and future directions. J. Clin. Oncol., *14:* 1383–1400, 1996.

2. Carrasquillo, J. A. Radioimmunotherapy of leukemia and lymphoma. *In:* H. Wagner (ed.), Principles of Nuclear Medicine, 2nd ed., pp. 1117–1132. Philadelphia: W. B. Saunders, 1996.

3. Waldmann, T. A., White, J. D., Carrasquillo, J. A., Reynolds, J. C., Paik, C. H., Bansow, O. A., Brechbiel, M. W., Jaffe, E. S., Fleisher, T. A., and Goldman, C. K. Radioimmunotherapy of interleukin-2R α-expressing adult T-cell leukemia with yttrium-90-labeled anti-Tac. Blood, *86:* 4063–4075, 1995.

4. Press, O. W., Eary, J. F., Appelbaum, F. R., Martin, P. J., Nelp, W. B., Glenn, S., Fisher, D. R., Porter, B., Matthews, D. C., Gooley, T., *et al.* Phase II trial of ^{131}I-B1 (anti-CD20) antibody therapy with autologous stem cells transplantation for relapsed B cell lymphomas. Lancet, *346:* 336–340, 1995.

5. Kaminski, M. S., Zasadny, K. R., Francis, I. R., Milik, A. W., Ross, C. W., Moon, S. D., Crawford, S. M., Burgess, J. M., Petry, N. A., Butchko, G. M., Gleen, S. D., and Wahl, R. L. Radioimmunotherapy of B-cell lymphoma with ^{131}I-anti-B1 (anti-CD20) antibody. N. Engl. J. Med., *329:* 459–465, 1993.

6. DeNardo, G. L., and DeNardo, S. J. Treatment of B-lymphocyte malignancies with ^{131}I-Lym-1 and ^{67}CU-2IT-BAT-Lym-1 and opportunities for improvement. *In:* D. M. Goldenberg (ed.), Cancer Therapy with Radiolabeled Antibodies, pp. 217–227. Boca Raton, FL: CRC Press, 1995.

7. Murray, J. L., Macey, D. J., Kasi, L. P., Rieger, P., Cunningham, J., Bhadkamkar, V., Shang, H. Z., Scholm, J., Rosenblum, M. G., and Podoloff, D. A. Phase II radioimmunotherapy trial with ^{131}I-CC49 in colorectal cancer. Cancer (Phila.), *73:* 1057–1066, 1994.

8. Meredith, R. F., Bueschen, A. J., Khazaeli, M. B., Plott, W. E., Grizzle, W. E., Wheeler, R. H., Schlom, J., Russell, C. D., Liu, T., and Lobuglio, A. F. Treatment of metastatic prostate carcinoma with radiolabeled antibody CC49. J. Nucl. Med., *35:* 1017–1022, 1994.

9. Begent, R. H., Ledermann, J. A., Green, A. J., Bagshawe, K. D., Riggs, S. J., Searle, F., Keep, P. A., Adam, T., Dale, R. G., and Glaser, M. G. Antibody distribution and dosimetry in patients receiving radiolabeled antibody therapy for colorectal cancer. Br. J. Cancer, *60:* 406–412, 1989.

10. Fujimori, K., Covell, D. G., Fletcher, J. E., and Weinstein, J. N. A modeling analysis of monoclonal-antibody percolation through tumors: a binding-site barrier. J. Nucl. Med., *31:* 1191–1198, 1990.

11. Zhu, H., Baxter, L. T., and Jain, R. K. Potential and limitations of radioimmuno-detection and radioimmunotherapy with monoclonal antibodies. J. Nucl. Med., *38:* 731–741, 1997.

12. Mausner, L. F., and Srivastava, S. C. Selection of radionuclides for radioimmunotherapy. Med. Phys., *20:* 503–509, 1993.

13. Pastan, I., Lovelace, E. T., Gallo, M. G., Rutherford, A. V., Magnani, J. L., and Willingham, M. C. Characterization of monoclonal antibodies B1 and B3 that react with mucinous adenocarcinomas. Cancer Res., *51:* 3781–3787, 1991.

14. Pai, L. H., Wittes, R., Setser, A., Willingham, M. C., and Pastan, I. Treatment of advanced solid tumors with immunotoxin LMB-1: an anti-Lewis^{Y} antibody linked to recombinant PE38. Nat. Med., *2:* 350–353, 1996.

15. Camera, L., Kinuya, S., Pai, L. H., Garmestani, K-h., Brechbiel, M. W., Gansow, O. A., Paik, C. H., Pastan, I., and Carrasquillo, J. A. Pre-clinical evaluation of ^{111}In-labeled B3 monoclonal antibody: biodistribution and imaging studies in nude mice bearing human epidermoid carcinoma xenografts. Cancer Res., *53:* 2834–2839, 1993.

16. Camera, L., Kinuya, S., Garmestani, K., Brechbiel, M. W., Wu, C., Pai, L. H., McMurry, T. J., Gansow, O. A., Pastan, I., Paik, C. H., and Carrasquillo, J. A. Comparative biodistribution of indium- and yttrium-labeled B3 monoclonal antibody conjugated to either 2-(p-SCN-Bz)-6-methyl-DTPA (1B4M-DTPA) or 2-(p-SCN-Bz)-1,4,7,10-tetraazacyclododecane tetraacetic acid (2B-DOTA). Eur. J. Nucl. Med., *21:* 640–646, 1994.

17. Camera, I., Kinuya, S., Garmestani, K., Brechbiel, M. W., Wu, C., Pai, L. H., McMurry, T. J., Gansow, O. A., Pastan, I., Paik, C. H., and Carrasquillo, J. A. Evaluation of the serum stability and *in vivo* biodistribution of CH-DTPA and other ligands for yttrium labeling of monoclonal antibodies. J. Nucl. Med., *35:* 882–889, 1994.

18. Naruki, Y., Carrasquillo, J. A., Reynolds, J. C., Maloney, P. J., Frincke, J. M., Neumann, R. D., and Larson, S. M. Differential cellular catabolism of ^{111}In, ^{90}Y- and ^{125}I-radiolabeled T101 anti-CD5 monoclonal antibody. Int. J. Radiat. Appl. Instrum. Part B, *17:* 201–207, 1990.

19. Carrasquillo, J. A., Mulshine, J. L., Bunn, P. A., Jr., Reynolds, J. C., Foon, K. A., Schroff, R. W., Perentesis, P., Steis, R. H., Keenan, A. M., Horowitz, M., *et al.* Indium-111 T101 monoclonal antibody is superior to iodine-131 T101 in imaging of cutaneous T-cell lymphoma. J. Nucl. Med., *28:* 281–287, 1987.

20. Chinol, M., and Hnatowich, D. J. Generator-produced yttrium-90 for radioimmunotherapy. J. Nucl. Med., *28:* 1465–1470, 1987.

21. Stewart, J. S., Hird, V., Snook, D., Sullinvan, M., Myers, M. J., and Epenetos, A. A. Intra-peritoneal ^{131}I- and ^{90}Y-labeled monoclonal antibodies for ovarian cancer: pharmacokinetics and normal tissue dosimetry. Int. J. Cancer, *3* (Suppl.)*:* 71–76, 1988.

22. Press, O. W., Shan, D., Howell-Clark, J., Eary, J., Appelbaum, F. R., Matthews, D., King, D. J., Haines, A. M., Hamann, P., Hinman, L., Shochat, D., and Bernstein, I. D. Comparative metabolism and retention of iodine-125, yttrium-90, and indium-111 radioimmunoconjugates by cancer cells. Cancer Res., *56:* 2123–2129, 1996.

23. Hnatowich, D. J., Snook, D., Rowlinson, G., Stewart, S., and Epenetos, A. A. Preparation and use of DTPA-coupled antitumor antibodies radiolabeled with yttrium-90. Targeted Diagn. Ther. Ser., *1:* 353–374, 1988.

24. Harrison, A., Walker, C. A., Parker, D., Jankowski, K. J., Cox, J. P., Craig, A. S., Sansom, J. M., Beeley, N. R., Boyce, R. A., Chaplin, L., *et al.* The *in vivo* release of ^{90}Y from cyclic and acyclic ligand-antibody conjugates. Int. J. Radiat. Appl. Instrum. Part B, *18:* 469–476, 1991.

25. Maecke, H. R., Riesen, A., and Ritter, W. The molecular structure of indium-DTPA. J. Nucl. Med., *30:* 1235–1239, 1989.

26. Cotton, F. A., and Wilkinson, G. Advanced Inorganic Chemistry, 5th ed. New York: John Wiley, 1988.

27. Gansow, O. A. Newer approaches to the radiolabeling of monoclonal antibodies by use of metal chelates. Int. J. Radiat. Appl. Instrum. Part B, *18:* 369–381, 1991.

28. Roselli, M., Schlom, J., Gansow, O. A., Raubitschek, A., Mirzadeh, S., Brechbiel, M. W., and Colcher, D. Comparative biodistributions of yttrium- and indium-labeled monoclonal antibody B72.3 in athymic mice bearing human colon carcinoma xenografts. J. Nucl. Med., *30:* 672–682, 1989.

29. Carrasquillo, J. A., White, J. D., Paik, C. H., Raubitschek, A., Le, N., Rotman, M., Brechbiel, M. W., Gansow, O. A., Top, L. E., Perentesis, P., Reynolds, J. C., Nelson, D. L., and Waldmann, T. A. Similarities and differences in distribution between ^{111}In and ^{90}Y 1B4M-DTPA labeled anti-Tac monoclonal antibody. J. Nucl. Med., *40:* 267–276, 1999.

30. DeNardo, S. J., Kramer, E. L., O'Donnell, R. T., Richman, C. M., Salako, Q. A., Shen, S., Noz, M., Glenn, S. D., Ceriani, R. L., and De Nardo, G. L. Radioimmunotherapy for breast cancer using indium-111/yttrium-90 BrE-3: results of a Phase I clinical trial. J. Nucl. Med., *38:* 1180–1185, 1997.

31. Knox, S. J., Goris, M. L., Trisler, K., Negrin, R., Davis, T., Liles, T. M., Grillo-Lopez, A., Chinn, P., Varns, C., Ning, S. C., Fowler, S., Deb, N., Becher, M., Marquez, C., and Levy, R. Yttrium-90-labeled anti-CD20 monoclonal antibody therapy of recurrent B-cell lymphoma. Clin. Cancer Res., *2:* 457–470, 1996.

32. Wiseman, G. A., Solinger, A. M., and Grillo-Lopez, A. IDEC-Y2B8 (Y-90 conjugated anti-CD20) dosimetry calculated from In-111 anti-CD20 in patients with low and intermediate grade B-cell non-Hodgkin's lymphoma (NHL) emphasis on bone marrow (BM). Blood, *90* (Suppl.)*:* 2273–2273, 1997.

33. Lindmo, T., Boven, E., Cuttitta, F., Fedorko, J., and Bunn, P. A., Jr. Determination of the immunoreactive fraction of radiolabeled monoclonal antibodies by linear extrapolation to binding at infinite antigen excess. J. Immunol. Methods, *72:* 77–89, 1984.

34. Recommended methods for measurement of red-cell and plasma volume: International Committee for Standardization in Haematology. J. Nucl. Med., *21:* 793–800, 1980.

35. Gibaldi, M. Biopharmaceutics and Clinical Pharmacokinetics, 3rd ed. Philadelphia: Lea & Febiger, 1984.

36. Loevinger, R., and Berman, M. Calculating the absorbed dose from biologically distributed radionuclides. MIRD Pamphlet #1. New York: The Society of Nuclear Medicine, 1976.

37. Ellis, R. E. The distribution of active bone marrow in the adult. Phys. Med. Biol., *5:* 255–258, 1961.

38. Sgouros, G., Jureidini, I. M., Scott, A. M., Graham, M. C., Larson, S. M., and Scheinberg, D. A. Bone marrow dosimetry: regional variability of marrow-localizing antibody. J. Nucl. Med., *37:* 695–698, 1996.

39. Reynolds, J. C., Del Vecchio, S., Sakahara, H., Lora, M. E., Carrasquillo, J. A., Neumann, R. D., and Larson, S. M. Anti-murine antibody response to mouse monoclonal antibodies: clinical findings and implications. Int. J. Radiat. Appl. Instrum. Part B, *16:* 121–125, 1989.

40. Lloyd, K. O., and Old, L. J. Human monoclonal antibodies to glycolipids and other carbohydrate antigens: dissection of the humoral immune response in cancer patients. Cancer Res., *49:* 3445–3451, 1989.

41. Tolcher, A. W., Sugarman, S., Gelmon, K. A., Cohen, R., Saleh, M., Isaacs, C., Young, L., Healey, D., Onetto, N., and Slichenmyer, W. Randomized Phase II study of BR96-doxorubicin conjugate in patients with metastatic breast cancer. J. Clin. Oncol., *17:* 478–484, 1999.

42. Abdel-Nabi, H. H., Schwartz, A. N., Higgano, C. S., Wechter, D. G., and Unger, M. W. Colorectal carcinoma: detection with In-111 anti-carcinoembryonic-antigen monoclonal antibody ZCE-025. Radiology, *164:* 617–621, 1987.

43. Patt, Y. Z., Lamki, L. M., Haynie, T. P., Unger, M. W., Rosenblum, M. G., Shirkhoda, A., and Murray, J. L. Improved tumor localization with increasing dose of indium-111-labeled anti-carcinoembryonic antigen monoclonal antibody ZCE-025 in metastatic colorectal cancer. J. Clin. Oncol., *6:* 1220–1230, 1988.

44. Welt, S., Divgi, C. R., Real, F. X., Yeh, S. D., Garin-Chesa, P., Finstad, C. L., Sakamoto, J., Cohen, A., Sigurdson, E. R., and Kemeny, N. Quantitative analysis of antibody localization in human metastatic colon cancer: a Phase I study of monoclonal antibody A33. J. Clin. Oncol., *8:* 1894–1906, 1990.

45. Vriesendorp, H. M., Herpst, J. M., Germack, M. A., Klein, J. L., Leichner, P. K., Loudenslager, D. M., and Order, S. E. Phase I–II studies of yttrium-labeled antiferritin treatment for end-stage Hodgkin's disease, including Radiation Therapy Oncology Group 87-01. J. Clin. Oncol., *9:* 918–928, 1991.

46. Deb, N., Goris, M., Trisler, K., Saal, J., Ning, S., Becker, M., Marquez, C., and Knox, S. Treatment of hormone-refractory prostate cancer with 90Y-CYT-356 monoclonal antibody. Clin. Cancer Res., *2:* 1289–1297, 1996.

47. Leichner, P. K., Alabani, G., Colcher, D., Harrison, K. A., Hawkins, W. G., Eckblade, M., Baranowska-Kortylewicz, J., Augustine, S. C., Wisecarver, J., and Tempero, M. A. Patient-specific dosimetry of indium-111- and yttrium-90-labeled monoclonal antibody CC49. J. Nucl. Med., *38:* 512–516, 1997.

48. Foss, F. M., Raubitscheck, A., Mulshine, J. L., Fleisher, T. A., Reynolds, J. C., Paik, C. H., Neumann, R. D., Boland, C., Perentesis, P., Brown, M. R., Frincke, J. M., Lollo, C. P., Larson, S. M., and Carrasquillo, J. A. Phase I study of the pharmacokinetics of a radioimmunoconjugate, ^{90}Y-T101, in patients with CD5-expressing leukemia and lymphoma. Clin. Cancer Res., *4:* 2691–2700, 1998.

49. Schrier, D. M., Stemmer, S. M., Johnson, T., Kasliwal, R., Lear, J., Matthes, S., Taffs, S., Dufton, C., Glenn, S. D., Butchko, G., Ceriani, R. L., Rovira, D., Bunn, P., Shpall, E. J., Bearman, S. I., Purdy, M., Cagnoni, P., and Jones, R. B. High-dose ^{90}Y Mx-diethylenetriaminepentaacetic acid (DTPA)-BrE-3 and autologous hematopoietic stem cell support (AHSCS) for the treatment of advanced breast cancer: a Phase I trial. Cancer Res., *55* (Suppl.)*:* 5921s–5924s, 1995.

50. White, C. A., Halpern, S. E., Parker, B. A., Miller, R. A., Hupf, H. B., Shawler, D. L., Collins, H. A., and Royston, I. Radioimmunotherapy of relapsed B-cell lymphoma with yttrium 90 anti-idiotype monoclonal antibodies. Blood, *87:* 3640–3649, 1996.

51. Wong, J. Y., Williams, L. E., Yamauchi, D. M., Odom-Maryon, T., Esteban, J. M., Neumaier, M., Wu, A. M., Johnson, D. K., Primus, F. J., Shively, J. E., *et al.* Initial experience evaluating ^{90}yttrium-radiolabeled anti-carcinoembryonic antigen chimeric T84.66 in a Phase I radioimmunotherapy trial. Cancer Res., *55* (Suppl.)*:* 5929s–5934s, 1995.

52. Leichner, P. K., Akabani, G., Colcher, D., Harrison, K. A., Hawkins, W. G., Eckblade, M., Baranowski-Kortylewicz, J., Augustine, S. C., Wisecarver, J., and Tempero, M. A. Patient-specific dosimetry of indium-111- and yttrium-90-labeled monoclonal antibody CC49. J. Nucl. Med., *38:* 512–516, 1997.

53. Halpern, S. E., Haindl, W., Beauregard, J., Hagan, P., Clutter, M., Amox, D., Merchant, B., Unger, M., Mongovi, C., and Bartholomew, R. Scintigraphy with In-111-labeled monoclonal antitumor antibodies: kinetics, biodistribution and tumor detection. Radiology, *168:* 529–536, 1988.

54. Press, O. W., Eary, J. F., Appelbaum, F. R., and Bernstein, I. D. Myeloablative radiolabeled antibody therapy with autologous bone marrow transplantation for relapsed B cell lymphomas. Cancer Treat. Res., *76:* 281–297, 1995.

55. Richman, C. M., DeNardo, S. J., O'Grady, L. F., and DeNardo, G. L. Radioimmunotherapy for breast cancer using escalating fractionated doses of ^{131}I-labeled chimeric antibody with peripheral blood progenitor cell transfusions. Cancer Res., *55* (Suppl.)*:* 5916s–5920, 1995.

56. Stewart, J. S. W., Hird, V., Snook, D., Dhokia, B., Sivolapenko, G., Hooker, G., Papadimitriou, J. T., Rowlinson, G., Sullivan, M., Lambert, H. E., *et al.* Intraperitoneal yttrium-90 labeled monoclonal antibody in ovarian cancer. J. Clin. Oncol., *8:* 1941–1950, 1990.

Clinical Cancer Research

Imaging and Phase I Study of ^{111}In- and ^{90}Y-labeled Anti-Lewis ^{Y} Monoclonal Antibody B3

Lee H. Pai-Scherf, Jorge A. Carrasquillo, Chang Paik, et al.

Clin Cancer Res 2000;6:1720-1730.